AIChE WILEY InterScience DISCOVER SOMETHING GREAT

REACTORS, KINETICS, AND CATALYSIS

Kinetic Parameter Analysis for Propane ODH: V_2O_5/Al_2O_3 and MoO_3/Al_2O_3 Catalysts

T. V. Malleswara Rao and Goutam Deo
Dept. of Chemical Engineering, Indian Institute of Technology Kanpur, Kanpur 208 016, India

DOI 10.1002/aic.11176
Published online April 11, 2007 in Wiley InterScience (www.interscience.wiley.com).

The effect of surface metal oxide loading and specific surface metal oxide species on the kinetic parameters associated with the propane oxidative dehydrogenation reaction is analyzed for several supported V_2O_5/Al_2O_3 (VAl) and MoO_3/Al_2O_3 (MoAl) catalysts. The VAl and MoAl catalysts are synthesized and characterized to ensure the kinetic parameters are estimated primarily for the surface metal oxide phase. The kinetic parameters are successfully estimated for a consecutive Mars–van Krevelen reaction model. Analysis of the parameters reveals that the apparent pre-exponential factors for propene formation and degradation reactions increase with loading for both VAl and MoAl catalysts up to monolayer coverage with the VAl possessing larger values. However, the relative increase of the individual apparent pre-exponential factors is different. The activation energy for propene formation is relatively invariant and does not contribute to the activity comparison. The difference in activation energies for propene formation and degradation decreases with surface vanadia loading, but is relatively similar with surface molybdena loading. Detailed analysis of the kinetic parameters conclusively reveals that the surface vanadia species provides a better active site in terms of activity and propene yield for the propane ODH reaction. © 2007 American Institute of Chemical Engineers *AIChE J,* 53: 1538–1549, 2007
Keywords: propane, ODH, vanadia, molybdena, alumina, activity, selectivity, yield, kinetic parameters

Introduction

Oxidative Dehydrogenation (ODH) of alkanes has been recognized as a potential route for the conversion of lower alkanes (ethane, propane, and butanes) into their corresponding alkenes.[1–5] For alkane ODH reactions invariably there exists a conversion-selectivity relationship that is detrimental to the formation of the desired product, the alkene. It is desirable that a catalyst is developed that provides a suitable conversion-selectivity relationship.

Supported metal oxide-based catalysts have been widely studied for alkane ODH reactions with the aim of enhancing the conversion-selectivity relationship. Among them, vanadium and molybdenum-oxide based catalysts have been effectively applied for the propane ODH reaction.[6–29] Much research has focused on understanding these supported metal oxide catalysts by correlating the catalytic activity with spectroscopic information.[5–11] Specifically, the catalytic performance of V_2O_5/Al_2O_3 and MoO_3/Al_2O_3 catalysts have been tested for propane ODH reaction to study the effect of metal oxide loading and modifiers.[12–22] However, to compare the different catalysts and, consequently, defining the role of the specific surface metal oxide species and the loading on the propene selectivity or yield it is necessary to develop an appropriate criterion. For example, comparisons achieved at similar contact times are not always appropriate since the conversions may be different. Another method is to compare the catalysts at the same conversion level. Though this

Correspondence concerning this article should be addressed to G. Deo at goutam@iitk.ac.in.

method has its merits comparison at the same conversion level does not provide an overall picture. To overcome this drawback comparison of catalysts can be achieved by analyzing the different kinetic parameters estimated for a common reaction mechanism. For example, recently it has been shown that different supported vanadium oxide catalysts may be compared by analyzing the different kinetic parameters.[30]

A few studies exist to understand the variations in various kinetic parameters involved in the propane ODH reaction over V_2O_5/Al_2O_3 and MoO_3/Al_2O_3 catalysts based on pseudo-first order reactions.[13,14,20] Additionally, Bottino et al.[17] studied the propane ODH reaction over V_2O_5/Al_2O_3 catalysts considering only the propene formation reaction from the mechanistic point of view.

The underlying requirement for the proper comparison of catalysts through kinetic parameter estimation is the use of a reaction model that explains the conversion and selectivity/yield data. Previous studies suggest that the Mars–van Krevelen (MVK) redox mechanism on reducible supported and mixed metal oxide catalysts is appropriate for describing the propane ODH reaction.[10–12,23–28] For example, transient isotopic studies for the propane ODH reaction over V_2O_5/ZrO_2[10] and Al_2O_3-supported $VCrMnXO_x$ mixed oxide[11] catalysts confirmed that the reaction kinetics are consistent with a Mars–van Krevelen reaction model. It was observed that propene is formed as a primary product and carbon oxides are mainly formed via consecutive propene oxidation. However, a minor contribution of direct propane combustion to carbon oxides does exist. Recently, it has been shown that the kinetic parameters estimated for a sequential Mars–van Krevelen (MVK) reaction model, considering propene as a primary product and carbon oxides as secondary combustion products are effective in explaining the propane ODH reaction over supported vanadium oxide catalysts.[12,24,30]

In the present study, for comparison of catalysts based on surface metal oxide loading and specific surface metal oxide species a series of alumina supported vanadium and molybdenum oxide catalysts are prepared by incipient wetness impregnation method and characterized by various techniques. The prepared catalysts are then examined for the propane ODH reaction for which the kinetic parameters are estimated. On the basis of the kinetic parameters obtained, the effect of the surface metal oxide loading and the specific surface metal oxide phase is examined.

Experimental

Catalyst preparation

Supported V_2O_5/Al_2O_3 (VAl) and MoO_3/Al_2O_3 (MoAl) catalysts were prepared by the incipient-wetness impregnation technique on the pretreated Al_2O_3 (Condea, Purolox, SBA 200) support. The precursors used were a solution of ammonium metavanadate (NH_4VO_3) in oxalic acid for the VAl catalysts and ammonium heptamolybdate ($(NH_4)_6Mo_7O_{24}.4H_2O$, Aldrich, 99.98% purity) for the MoAl catalysts. The preparation of the supported VAl catalysts has been elaborated elsewhere.[12] For the supported MoAl catalysts, the Al_2O_3 support was initially pretreated with incipient volumes of double distilled water and then calcined gradually up to 873 K and kept there for 6 h. Incipient volumes of solutions containing predetermined amounts of precursor and the pretreated support were intimately mixed to prepare the catalysts with different loadings of molybdenum oxide. The mixture was kept in a dessicator overnight followed by drying at 383 K for 6 h, and at 473 K for another 6 h. Finally the samples were calcined at 873 K for 6 h. The prepared catalysts were denoted as **x**VAl and **x**MoAl, where **x** is the wt % loading corresponding to V_2O_5 and MoO_3, respectively.

Catalyst characterization

Surface Area. The surface areas of the samples were obtained by a multi-point BET method using N_2 adsorption data at 77 K. Degassing of the samples was realized by heating the samples at 423 K in flowing helium. The apparatus used for the measurements was a COULTER SA 3100 analyzer equipped with SA-VIEW^{TM} software.

X-ray Diffraction. Powder XRD patterns of the prepared catalysts were measured with a Seifert ISO-Debyeflex 2002 using Ni filtered Kα radiation from a Cu target ($\lambda = 1.44056$ Å).

Raman spectroscopy

The ambient Raman spectra of the prepared catalysts were obtained using a UV-visible Raman spectrometer system (Horbia–Jobin Yvon LabRam-HR) coupled with a confocal microscope, 2400/900 grooves/mm grating and a notch filter. The samples were excited with a 532 nm (visible) Yag double-diode pumped laser and the spectral resolution was $\sim$2 cm^{-1}. The scattered photons were directed into a single monochromator (JOBIN YVON, LABRAM-HR). A CCD detector (Jobin Yvon CCD-3000V) was used to collect the signal. Sample weights of $\sim$0.01 g were placed onto a glass slide below the confocal microscope. Additional details are given elsewhere.[31]

Temperature programmed reduction using hydrogen

The H_2-TPR measurements were performed in a Micromeritics Pulse Chemisorb 2705 apparatus. A sample weight of $\sim$0.02 to 0.05 g was taken in a U-shaped quartz reactor and pretreated. The pretreatment was achieved by heating the sample in a He gas flow (30 mL/min) at 473 K for 30 min. After cooling the sample to 300 K, a 5% H_2/Ar mixture flowing at 30 mL/min was introduced into the reactor for reduction measurements. The catalyst sample was heated to a final temperature of 1150 K at a ramping rate of 10 K/min. The hydrogen consumption was measured by a thermal conductivity detector. Known amounts of 5% H_2/Ar mixture were used for quantification purpose.

Reaction studies

The prepared catalysts were examined for the propane ODH reaction at atmospheric pressure in a vertical down-flow quartz reactor mounted in a tubular furnace. Details of the reactor are given elsewhere.[12] Prior to the reaction studies the catalyst samples were heated in a muffle furnace for 30 min at 673 K. A physical mixture of 0.02 to 0.25 g of the catalyst and required amount of inert quartz particles to form a bed height of 1 cm was loaded into the reactor. The temperature of the catalyst bed was measured by a thermocouple located just above the cata-

lyst bed and was controlled by a PID temperature controller (FUJI Micro-controller X Model PXZ 4). The flow-rates of reactant and inert gases (propane, O_2, and N_2) were adjusted through separate thermal mass flow controllers (Bronkhost Hi-Tec, Model F-201D FAC-22-V) to maintain specified propane to oxygen ratio and total flow rate. The reactant gases were mixed prior to sending to the reactor. Nitrogen was used as a diluent and its amount was fixed corresponding to inlet air composition. The exit gases were sent for online analysis to a gas chromatograph (AIMIL-NUCON 5700) equipped with a methanizer. The carbon oxides (CO and CO_2) and hydrocarbons (C_3H_8 and C_3H_6) were separated using a Hysep-Q column and analyzed in FID mode.

The effect of contact time on propane conversion was studied at 653 K and a C_3H_8/O_2 ratio of 2:1 by changing the total reactant flow rate between 30 and 120 mL/min. For determining kinetic parameters the catalyst was initially heated in the reactor to 613 K in flowing O_2. After 30 min the required flow rate of C_3H_8, O_2, and N_2 was introduced for a C_3H_8/O_2 ratio of 1:1 and the temperature was varied from 613 to 673 K. After collecting the reaction data at the various temperatures, the inlet gas stream was changed to pure O_2 and then catalyst was heated at 613 K. After 30 min the inlet gas stream was changed and the propane ODH reaction was carried out at a C_3H_8/O_2 ratio of 2:1 by varying the temperatures from 613 to 673 K. Similarly the reaction data were obtained at C_3H_8/O_2 ratio of 3:1 after treatment of the catalyst at 613 K in flowing O_2 for 30 min. After collecting the data at all specified C_3H_8/O_2 ratios and temperatures, the reproducibility of some runs were verified. A constant total flow rate of 75 mL/min was maintained.

Runs were conducted in the absence of catalyst and no significant conversions were observed under the present experimental conditions. Low propane conversions were maintained to facilitate kinetic parameter estimation. For each catalyst several runs were taken at a particular temperature and the average value was used. The standard deviation of the data was less than 1.5%. On the basis of the inlet and outlet concentrations the activity, conversion, selectivity, yield, and TOF (turn over frequency) were calculated based on formulae given elsewhere.[32] The effects of interphase, interparticle, intraparticle diffusion, and heat transfer limitations were considered by applying published criteria[33] and none were found.

Kinetic parameter estimation

Several assumptions are made in developing the mathematical model for a fixed-bed plug flow reactor containing the catalyst.[12] These assumptions are justified since low propane conversions are maintained and nitrogen and inert quartz particles are used as diluents. On the basis of these assumptions the differential material balance equation for each component, i, in a plug flow reactor is

$$\frac{dx_i}{dW} = \frac{\sum_j n_{ij} r_j}{F_0} \tag{1}$$

where x_i is the mole fraction of the i^{th} component, W is the weight of the catalyst in g, F_0 is the total volumetric flow rate of the feed, in mL/min, n_{ij} is stoichiometric coefficient of the i^{th} component for the j^{th} reaction, and r_j is the rate of the j^{th} reaction.

The set of ordinary differential equations given in Eq. 1 can be solved to obtain the predicted output mole fraction of each component based on the input mole fraction of the component, x_{i0}, and knowledge of r_j, W, n_{ij}, F_0, temperature, and pressure of the reaction. The reaction rate, r_j, depends on the specific reaction-model considered. The reaction rates of a particular reaction-model contains several nonlinear kinetic parameters, θ_j, and some or all mole fractions, x_i, and is described below. Thus, the predicted output mole fractions are obtained by integrating the reaction rates over the entire mass based on a chosen reaction model. A fourth order Runge–Kutta method is employed for integrating the reaction rate expressions, r_j.

The output mole fraction of carbon containing compounds that are detected, C_3H_8, C_3H_6, CO, and CO_2, are assumed to be well represented by a nonlinear model given by

$$Y_h = g_h(\theta, X) + Z_h; \quad h = 1, 2, \ldots, v \tag{2}$$

where Y_h is the vector of random variables representing the response or the observed output variable, Z_h is the vector of errors associated while calculating the response, v is number of responses, which are the four carbon containing compounds, CO, CO_2, C_3H_6, and C_3H_8, $g_h(\theta, X)$ is the predicted output concentration, θ is the parameter vector and X is the vector of experimental variables (i.e., input mole fractions of components and temperature)

The predicted output mole fraction, g_h, obtained this way can then be compared with the actual output mole fraction, Y_h, based on the kinetic parameter values.

For multi-response systems and when responses are correlated, minimization of a determinant is ideally suited for comparing the predicted and actual output mole fractions.[34] During the minimization process the kinetic parameters are chosen such that the least value of the determinant is obtained.[12]

The determinant that is minimized for multiresponse systems

$$= |Z_{hk}| \tag{3}$$

$$\text{where,} \quad Z_{hk} = \sum_{u=1}^{n} (y_{hu} - g_{hu})(y_{ku} - g_{ku}) \; ; \; h \text{ and } k = 1, \ldots, v \tag{4}$$

n is the number of experiments, y_{hu} and y_{ku} are the experimental mole fractions of h^{th} and k^{th} components in u^{th} experiment, g_{hu} and g_{ku} are the predicted mole fractions of h^{th} and k^{th} components in u^{th} experiment, and v is the number of responses.

In the present study, minimization of the objective function given by Eq. 3 is achieved by applying a genetic algorithm (GA) for determining the kinetic parameters. The genetic algorithms are effective search techniques for optimization because of their global perspective. The use of GA with appropriate termination criteria, which include defining a proper fitness function and usage of proper termination conditions (for example, number of generations and reaching

Table 1. GA Parameters Used in the Present Study

GA Parameters	Values for MVK Model
Generations	4000 to 30000
Population size	100 to 300
Crossover probability	0.8
Mutation probability	0.2
Tournament size	2
Exponent for simulated binary crossover	2
Exponent for mutation	200
Seed value	0.2

a constant value of highest ranking solution's fitness value), nearly leads to a global solution. This has been confirmed for several optimization problems.[23] and references therein However, the nature of the solution does depend on the complexity of the problems. Furthermore, in our preliminary studies, we have also checked the nature of the solution obtained or parameters estimated from GA by taking them as initial guesses for further optimization using Levenberg–Marquardt algorithm. However, we do not see any improvement in the solution and is same as it obtained by GA. This suggests that the parameters estimated by GA are indeed globally optimized. The details of GA used in this study have been reported elsewhere.[23] The parameters used in the GA code are given in Table 1.

The kinetics of the propane ODH reaction for the present study can be represented by a MVK model built on a consecutive reaction scheme. The MVK reaction model suggests that the catalyst operates in two steps[35] and have been successfully applied for hydrocarbon oxidation over metal oxide catalysts.[26,36–38] In the first step the alkane molecule reacts with the lattice oxygen to form the products and in the second step the lattice oxygen of the catalysts is replenished by the gas phase oxygen. The rate of reaction is, thus, proportional to the alkane partial pressure and the concentration of oxidized sites and the rate of catalyst re-oxidation or lattice oxygen replenishment is proportional to the oxygen partial pressure and concentration of reduced sites. Accordingly the MVK mechanism chosen for this study assumes that the propane molecules react with lattice oxygen of the catalyst to produce propene molecules (r_1), which then reacts with lattice oxygen to produce CO (r_2) and CO_2 (r_3). Independent pathways are chosen for CO and CO_2 to facilitate proper determination of kinetic parameters. The gas phase oxygen replenishes the lattice oxygen by re-oxidation of the reduced catalyst (r_4).

Reactions r_1 to r_3 are part of the more generalized scheme suggested previously.[17,39]

The rate equations for the four reactions r_1 to r_4 are expressed as

$$r_1 = k_1 P_{C_3H_8}(1-\beta) \tag{5}$$

$$r_2 = k_2 P_{C_3H_6}(1-\beta) \tag{6}$$

$$r_3 = k_3 P_{C_3H_6}(1-\beta) \tag{7}$$

$$r_4 = k_4 P_{O_2}\beta \tag{8}$$

where β is the degree of reduction and is the fraction of the total active sites that are reduced at that particular reaction condition. According to the MVK reaction model, the rate of lattice-oxygen consumed in the reactions r_1 to r_3 equals the rate of lattice-oxygen replacement by the reaction r_4. Consequently, based on the stoichiometry, β is expressed as

$$\beta = \frac{0.5\,k_1\,P_{C_3H_8} + 3.0\,k_2\,P_{C_3H_6} + 4.5\,k_3\,P_{C_3H_6}}{0.5\,k_1\,P_{C_3H_8} + 3.0\,k_2\,P_{C_3H_6} + 4.5\,k_3\,P_{C_3H_6} + k_4\,P_{O_2}} \tag{9}$$

Furthermore, Eq. 9 reveals that β depends on various factors that include operating conditions and the catalytic systems studied. On the basis of the variation of the degree of reduction, the kinetic order of the propane ODH reaction rates will change.

To facilitate proper determination of kinetic parameters reparameterization is done to overcome the correlation between k_{i0} and E_i.[12,26] Reformulation is achieved by centering the rate constant about a mean temperature. Consequently, the rate constant is given by

$$k_i = k_{i0}\exp\left(\frac{-E_i}{R}\left(\frac{1}{T}-\frac{1}{T_m}\right)\right) \tag{10}$$

where k_i is the rate constant for the i^{th} reaction, in mL STP min^{-1} (g cat)$^{-1}$atm^{-1}, k_{i0} is the apparent pre-exponential factor or the rate constant at the mean reaction temperature, E_i is the activation energy for the reaction i, in kJ/mol, R is the universal gas constant, in kJ (kmol)$^{-1}$ K, T is the actual reaction temperature and T_m is the mean reaction temperature, in K.

Furthermore, standard error calculations of the kinetic parameters, k_{i0}'s and E_i's, are achieved by applying previously defined equations.[24]

Results and Discussion

Surface area

The surface areas of the Al_2O_3 support, VAl and MoAl samples were determined and tabulated in Table 2. It is observed

Table 2. Support and Catalyst Characteristics From Surface Area and TPR Studies

Catalyst	MoO_3 (wt %)	Surface Area (m^2/g)	Surface Density (atoms/nm^2)	H/Mo ($T_{max,1}$)	Catalyst	V_2O_5 (wt %)	Surface Area (m^2/g)	Surface Density (atoms/nm^2)	H/V ($T_{max,1}$)
Al_2O_3	0	180	0	–	5VAl	5	165	2.0	n.d
10MoAl	10	165	2.4	1.6	7.5VAl	7.5	159	3.1	1.9
15MoAl	15	157	4.0	1.7	10VAl	10	146	4.5	2.0
17.5MoAl	17.5	150	4.9	2.0	12.5VAl	12.5	134	6.2	2.0
20MoAl	20	142	5.9	2.0	15VAl	15	110	9.0	2.0
25MoAl	25	118	8.9	2.0	17.5VAl	17.5	n.d	n.d	2.0

n.d., not determined.
Surface density calculation is based on the surface area of the catalyst.

from Table 2 that the surface areas range from 110 to 180 m^2/g cat and decrease with increase in surface metal oxide loading. A decrease in surface area with surface metal oxide loading has been observed before and is usually associated with the blocking of the micropores of the support and/or difference in the atomic masses of vanadium/molybdenum with respect to aluminum. The surface densities of these supported catalysts are also calculated using Eq. 11 and are given in Table 2. The H/Mo and H/V values obtained from TPR experiments are also presented in Table 2 and are discussed later.

$$\text{Surface density (atoms/nm}^2) = \frac{\text{wt \% Metal Oxide loading} \times \text{No. of Metal atoms in } M_xO_y \times 6.023 \times 10^{23}}{\text{Molecular Weight of Metal Oxide} \times 100 \times \text{Surface Area}} \quad (11)$$

Ambient Raman spectroscopy and XRD pattern

The ambient Raman spectra of the supported VAl and MoAl catalysts are presented in the 200–1100 cm^{-1} region in Figure 1. Raman spectra of the supported VAl catalysts reveal that only molecularly-dispersed hydrated surface vanadia species[40,41] are present on the Al_2O_3 support up to 15 wt % loading. The molecularly dispersed surface metal oxide species was confirmed since the dehydrated Raman spectra were different from the spectra obtained under ambient conditions and also different from crystalline compounds. The dehydrated Raman spectra are not shown for brevity. The Raman spectrum of the 17.5VAl sample revel the presence of sharp bands associated with bulk $AlVO_4$.[31,42,43] The formation of $AlVO_4$ instead of bulk V_2O_5 for high loadings of V_2O_5/Al_2O_3 has been observed before.[42] The bulk $AlVO_4$ species detected by Raman spectroscopy is XRD amorphous since no diffraction patterns are observed in the powder pattern. The XRD patterns are not shown for brevity. Detection of surface vanadia species in the 17.5VAl sample is difficult due to strong $AlVO_4$ Raman bands.[42] The ambient Raman spectra of the MoAl samples reveal the presence of surface molybdena species on the alumina support.[44] For the 25 MoAl sample Raman bands due to bulk $Al_2(MoO_4)_3$ and surface molybdena species are observed.[44,45] The bulk $Al_2(MoO_4)_3$ is, however, not detected by XRD.

Interestingly, the presence of bulk V_2O_5 and MoO_3 in the VAl and MoAl samples at high vanadia or molybdena loadings is not observed. The presence of bulk V_2O_5 and MoO_3 in the Raman spectra provides the basis of monolayer coverage from which fractional coverage of a particular loading of metal oxides can be determined.[46] In the present study it appears that the bulk V_2O_5 and MoO_3 react with this Al_2O_3 support to form the corresponding $AlVO_4$ and $Al_2(MoO_4)_3$ compounds using the present synthesis methods. It has also been reported that at above 773 K bulk MoO_3 formed readily interacts with Al_2O_3 to form $Al_2(MoO_4)_3$ phase.[47] The presence of $AlVO_4$ and $Al_2(MoO_4)_3$ detected Raman spectra may also be due to local heating effects of the laser since the samples are stationary in contrast to Raman analysis on spinning samples.[46] The presence of the surface vanadia and molybdena species are, however, evident and the detection of the bulk compounds suggests loadings in excess of monolayer coverage. Furthermore, the highest surface density calculated for observing only surface metal oxide species correspond to 9.0 V and 5.9 Mo atoms/nm^2, which compares well with previous studies.[44,48] Thus, monolayer coverages of vanadia and molybdena correspond to 15 and 20%, respectively, and the different loadings of vanadia and molybdena can be represented as fractional coverages.

H_2-TPR studies

The H_2-TPR profiles obtained for the supported VAl and MoAl samples are presented in the 550 to 950 K temperature range in Figures 2a, b, respectively. In Figure 2a, a single reduction peak in the 700–800 K region is observed for the VAl samples, except for 17.5 Val, where an additional reduction peak is present at 867 K. Correlating with the Raman data it appears that the $AlVO_4$ species gives rise to this additional reduction peak. It can be seen from Figure 2b that for all the MoAl samples, except 10MoAl, multiple reduction peaks are observed below 950 K suggesting that reduction of the molybdena species occur through several stages.[49–51] In contrast, the TPR profile of the 10MoAl sample shows a single reduction step. The TPR profile of 25MoAl sample reveals an additional reduction peak at 793 K, which appears to correspond to the $Al_2(MoO_4)_3$ species observed by Raman spectroscopy.

Comparing the reducibility of the surface vanadia and molybdena species, represented by the T_{max} temperature, it appears that the surface metal oxide loading does not significantly change the T_{max} temperature, however the specific sur-

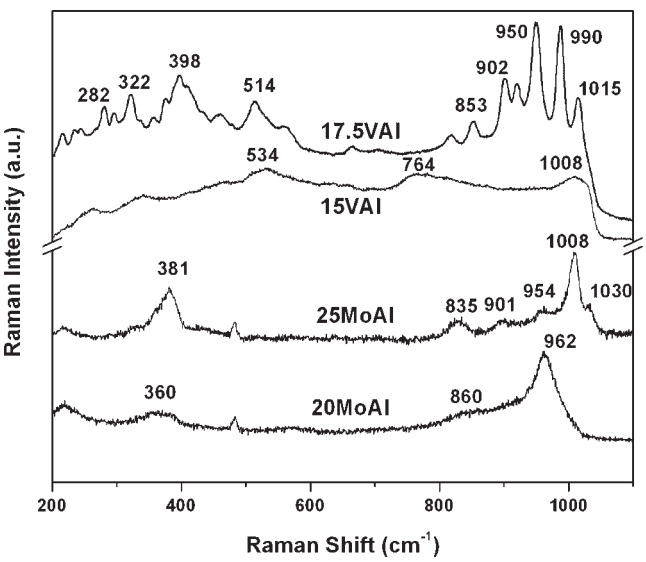

Figure 1. Ambient Raman Spectra of the supported VAl and MoAl catalysts.

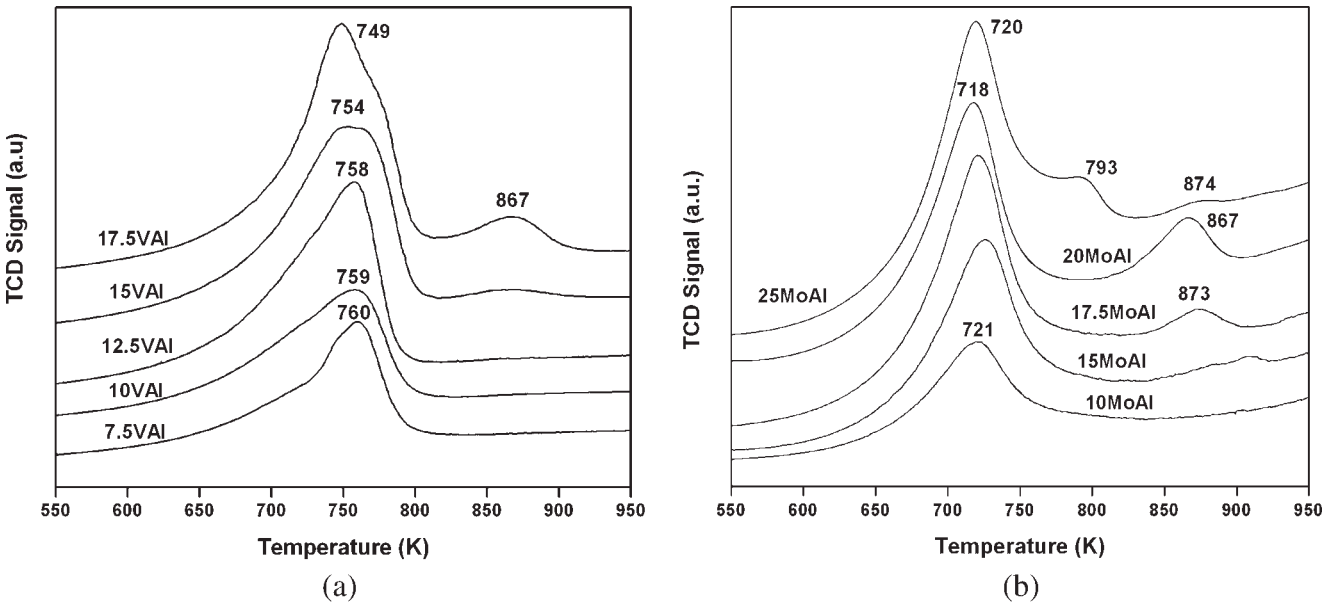

Figure 2. (a) TPR patterns of supported V_2O_5/Al_2O_3 catalysts. (b) TPR patterns of supported MoO_3/Al_2O_3 catalysts.

face metal oxide species does have a small influence on the T_{max} temperature. The first reduction temperature values (T_{max1}) for the MoAl samples range from 718 to 721 K, and are lower than those for the VAl samples, which range from 749 to 760 K.

On the basis of the integrated area of the reduction peaks the H/V and H/Mo values for T_{max}, were determined from TPR experiments and are listed in Table 2. A H/V value of ~2 is found for all VAl samples, which corresponds to the reduction of V^{+5} species to V^{+3} species.[12,42] For the MoAl samples, a H/Mo value of ~2 for the first reduction peak suggests that the surface Mo^{+6} oxide species are initially reduced to Mo^{+4} oxide species.[49–51] The H/Mo values are found to be slightly <2 for low molybdena loading.

Reaction studies and kinetic analysis

The propane ODH reaction studies were performed as a function of contact times at a C_3H_8:O_2 ratio of 2:1 and temperature of 653 K over the different VAl and MoAl samples and pure Al_2O_3 support. The results for the different catalysts and oxide support are presented in Figures 3a, b. The Al_2O_3 support possessed low propane ODH activity (conversion levels: 0.1–0.3%; propene selectivity ~57%), which is much

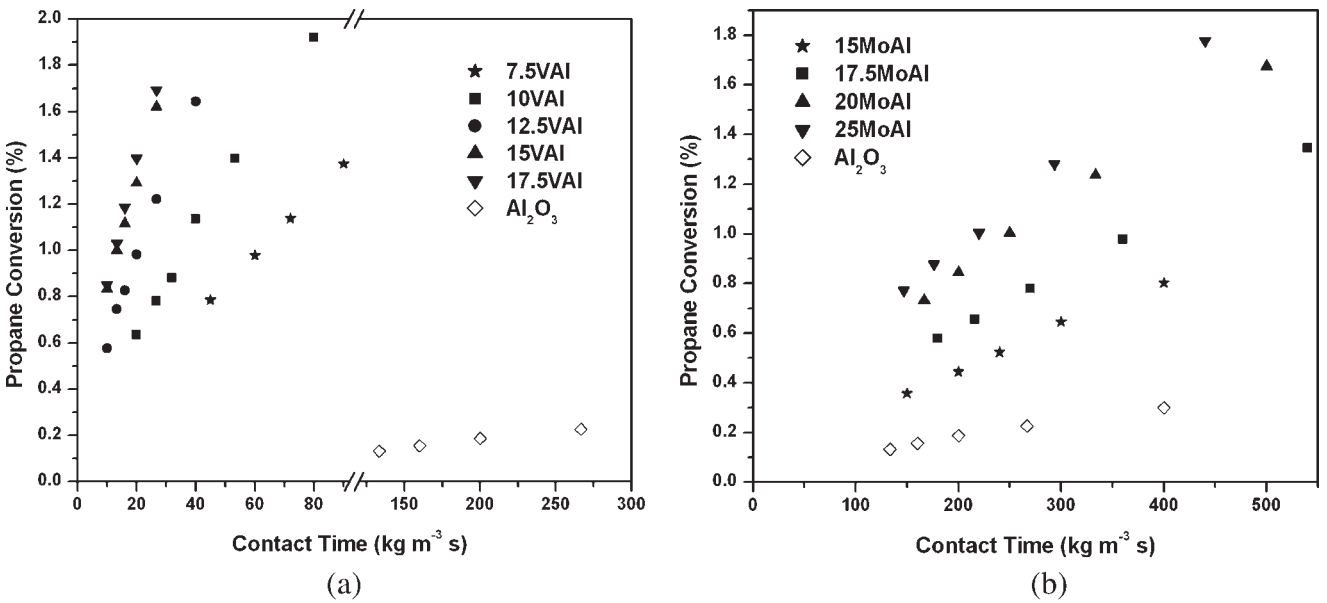

Figure 3. Variation of propane conversion with contact time for (a) VAl samples and (b) MoAl samples at T = 653 K and C_3H_8:O_2 = 2:1.

Table 3. Activity and Turn Over Frequency (TOF) Values of Supported VAl and MoAl Catalysts

Contact Time (kg m^{-3} s)	Catalysts	Experimental: Activity (gmol/g·s) × 10^6	Experimental: TOF (s^{-1}) × 10^3	TOF (s^{-1}) × 10^3 (Predicted)	Based on Eqs. (12) and (13): Term I (gmol/g·s) × 10^6	Based on Eqs. (12) and (13): Term II (gmol/g·s) × 10^6
20	10VAl	3.9	3.5	3.3	3.98	0.366
	12.5VAl	6.0	4.4	4.5	7.03	0.821
	15VAl	8.1	4.9	5.2	9.46	0.912
	17.5VAl	8.6	4.5	4.5	10.4	1.752
200	15MoAl	0.27	0.26	0.25	0.27	0.005
	17.5MoAl	0.38	0.32	0.35	0.45	0.023
	20MoAl	0.52	0.36	0.39	0.63	0.080
	25MoAl	0.59	0.35	0.38	0.73	0.082

Reaction conditions: $T = 653$ K, C_3H_8:$O_2 = 2$:1.

lower than the activity for the supported VAl and MoAl catalysts. Thus, the catalytic propane ODH activity observed is primarily due to the surface vanadia and molybdena species.

From Figures 3a, b it is observed that the propane conversion increases with an increase in contact time for all the samples considered. The propane conversion at iso-contact time is, however, a function of metal oxide loading and specific surface metal oxide species. For the VAl samples, the propane conversion at a particular contact time increases with vanadia loading up to 15VAl and is then relatively constant for the 17.5 VAl sample. Similar results are observed for the MoAl samples where the propane conversion increases up to 20MoAl and is then relatively constant for the 25MoAl sample. The relatively constant conversion for the high loading samples coincide with the formation of additional species ($AlVO_4$ or $Al_2(MoO_4)_3$) observed by the characterization techniques, which correspond to loading slightly in excess of monolayer coverage. On the basis of the conversion data the TOFs are calculated at a specific contact times for the VAl and MoAl catalysts and are presented in Table 3. The data in Table 3 reveals that the TOFs are relatively constant with an increase in loading. Previous studies have also observed invariant TOF values with increase in loading for the vanadium oxide species on Al_2O_3 support,[15] suggesting that the propane ODH reaction is structure insensitive. However, the TOF is a strong function of the specific metal oxide phase on Al_2O_3 support. The TOF for the VAl catalysts is more than an order of magnitude compared with that for the MoAl catalysts.

The variation of propene selectivity with propane conversion is shown in Figure 4 for the VAl and MoAl catalysts. It is clear from Figure 4 that the propene selectivity is inversely related to the conversion for each catalyst. Furthermore, as the surface metal oxide species and loading on Al_2O_3 are changed the specific propene selectivity-conversion curve is affected. It appears that the VAl samples (given in filled symbols) provide higher propene selectivity at iso-conversion compared with the MoAl samples. However, specific variations with loading are not evident.

To study the effect of loading and specific surface metal oxide phase in terms of the kinetic parameters some of the supported VAl and MoAl catalysts were considered for detailed analysis. The kinetic parameters of the catalysts are estimated for the MVK reaction model, and their values, units and the standard error associated with each kinetic parameter value are presented in Table 4. From Table 4 it is observed that the standard error values are small relative to the corresponding parameter values. To emphasis the efficacy of the model and the associated kinetic parameters the normalized actual and predicted concentrations are plotted in Figure 5. Since the concentrations of the carbon containing compounds are different it is necessary to normalize them so that the comparison between the actual and predicted concentrations can be done properly. The scaling is done by dividing the actual and predicted concentrations of component "i" by a constant value that is different for each component. The constant value is the highest concentration observed for that respective component. Figure 5 illustrates the quality of agreement between the actual and predicted concentrations of the carbon containing compounds analyzed (C_3H_8, C_3H_6, CO_2, and CO) for the 15VAl and 20MoAl samples suggesting proper representation of the reaction. Similar plots are also observed for the other catalysts and are not shown for brevity. Thus, proper representation of the propane ODH reaction over these alumina supported catalysts is achieved.

Detailed analysis of the kinetic parameters in Table 4 reveals that the primary apparent pre-exponential factor, k_{10}, of the VAl catalysts increases as the loading is increased up

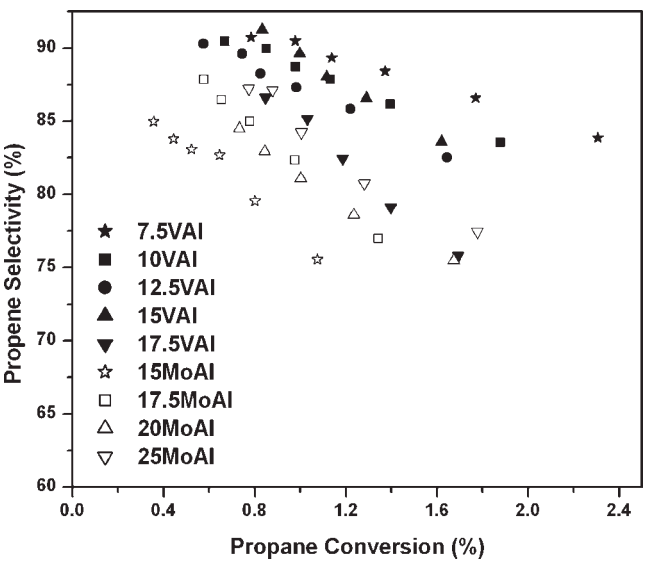

Figure 4. Variation of propene selectivity with propane conversion at $T = 653$ K and C_3H_8:$O_2 = 2$:1.

Table 4. Kinetic Parameters for Supported VAl and MoAl Catalysts

Parameters	Units	Parameter Values for the Catalysts								
		7.5VAl	10VAl	12.5VAl	15VAl	17.5VAl	15MoAl	17.5MoAl	20MoAl	25MoAl
k_{10}	mL STP min^{-1}	8.5 (0.2)	14.7 (0.5)	26 (0.4)	36 (0.3)	38 (0.5)	1.0 (0.01)	1.63 (0.01)	2.31 (0.1)	2.7 (0.03)
k_{20}	(g cat)$^{-1}$ atm^{-1}	75 (4)	171 (5)	287 (3)	366 (2)	565 (3)	20 (0.4)	32 (0.2)	33 (2)	31 (2)
k_{30}		65 (1)	139 (2)	188 (1)	209 (2)	295 (2)	26 (0.4)	34 (0.2)	42 (2)	35 (5)
k_{40}		54 (1)	205 (5)	307 (5)	484 (6)	395 (2)	74 (5)	52 (0.3)	29 (1)	39 (1)
E_1	kJ mol^{-1}	100 (1)	98 (1)	94 (1)	92 (1)	102 (2)	96 (1)	102 (1)	99 (1)	100 (3)
E_2		50 (4)	55 (4)	83 (2)	88 (2)	97 (1)	68 (2)	33 (1)	54 (3)	46 (5)
E_3		46 (1)	49 (2)	75 (2)	81 (1)	93 (1)	59 (1)	36 (1)	46 (1)	40 (7)
E_4		130 (2)	93 (2)	107 (9)	156 (3)	91 (2)	181 (16)	119 (2)	125 (5)	98 (4)

The standard errors are given in parentheses. $T_m = 643$ K.

to monolayer coverage (15VAl) and then increases gradually. Similar relative variations are observed for the MoAl samples. The gradual increase in k_{10} values for above monolayer value appears to be associated with the lower activity associated with bulk vanadates and molybdates. The k_{20} and k_{30} values for the VAl catalysts increase gradually till monolayer coverage (15VAl) and then increase rapidly for the 17.5VAl catalyst. It appears that the presence of bulk vanadates increase the k_{20} and k_{30} values. The k_{20} and k_{30} values for the MoAl samples increase up to 17.5MoAl and are then relatively constant for high surface coverage catalysts. In contrast to the VAl samples the k_{20} and k_{30} values of the bulk molybdates appear to be less active for CO_x formation.

Comparison of the different activation energies shown in Table 4 reveals that the activation energy for propene formation or propane oxidation, E_1, is relatively independent of metal oxide loading and specific surface metal oxide phase and range from 92–102 kJ/mol. The activation energies for CO and CO_2 formation, E_2 and E_3, are always less than E_1; and $E_2 \sim E_3$. For the VAl catalysts the activation energies for propene oxidation or carbon oxide formation reactions, E_2 and E_3, increase with an increase in metal oxide loading and approach a relatively constant value of ~90 kJ/mol. The difference between E_1 and E_2 or E_3 consequently decreases. For the MoAl catalysts, however, the activation energies, E_2 and E_3, are relatively constant at 33 to 54 and 36 to 46 kJ/mol, respectively. Variations in the catalyst re-oxidation kinetic parameters, k_{40} and E_4, are discussed later.

The increase in k_{10} values with an increase in metal oxide loading also indicate an increase in k_1 values since the propene formation activation energy is relatively constant for all the catalysts. Furthermore, the k_{10} and the corresponding k_1 values are larger for the VAl catalysts relative to the MoAl catalysts suggesting the inherent higher activity of the surface vanadia site. For comparing with the TOF data the k_{10} values of the VAl samples given in Table 4 are normalized per vanadia site and represented by k_{10}^*. The ratio of the k_{10}^* values is: $(k_{10}^*)_{10VAl} : (k_{10}^*)_{12.5VAl} : (k_{10}^*)_{15VAl} : (k_{10}^*)_{17.5VAl}$ ~1 : 1.4 : 1.6 : 1.5, where k_{i0}^* is given in terms of ml STP min^{-1} (g V)$^{-1}$ atm^{-1}. The trends in primary rate constant for propene formation, k_1 and k_{10} values and in the normalized rate constant k_1^* and k_{10}^* values are similar since the activation energy for propene formation, E_1, is similar. However, the ratio of TOF values given in Table 3 is slightly different from the ratio of the primary rate constants since the degree of reduction, β, at iso-contact time may vary. Normalizing the k_{10} values of the MoAl catalysts per molybdena site, as done previously, reveals that the ratio of k_{10}^* values is: $(k_{10}^*)_{15MoAl} : (k_{10}^*)_{17.5MoAl} : (k_{10}^*)_{20MoAl} : (k_{10}^*)_{25MoAl}$ ~1 : 1.4 : 1.8 : 1.6, which is also slightly different from the ratio of TOF values. Similar to the VAl catalysts the degree of reduction needs to considered with the k_{10}^* values to give a quantitative agreement with the ratio of the TOF values.

To appreciate the contribution of the degree of reduction on the reaction rates the degree of reduction, β, defined in Eq. 9, is evaluated for all the catalysts and is plotted as a function of contact time in Figure 6 at 653 K and a C_3H_8:O_2 ratio of 2:1. Figure 6 depicts the nonlinear increase in β with contact time for the different catalysts. It is clear from Figure 6 that at iso-contact time β is higher for the VAl catalysts than the MoAl catalysts. The primary reaction rate given by Eq. 5 depends on $(1 - \beta)$ and to compare the experimental TOF values for the different catalysts Eq. 5 is integrated from the contact time limits of zero to 20 or 200 kg m^{-3} s, converted as TOF and listed in Table 3 for the VAl and MoAl catalysts. Comparison of the experimental TOF and predicted TOF based on the kinetic parameters evaluated in Table 3 re-iterates the proper representation of the propane

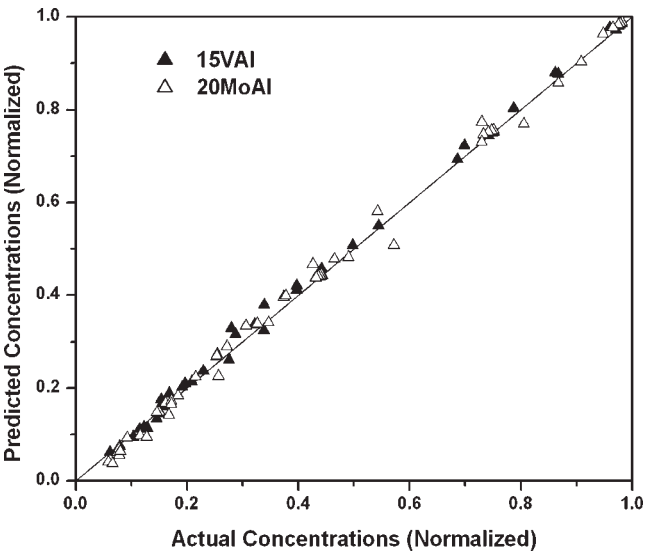

Figure 5. Comparison of the predicted and actual concentrations of all the carbon containing compounds for the 15VAl and 20MoAl samples.

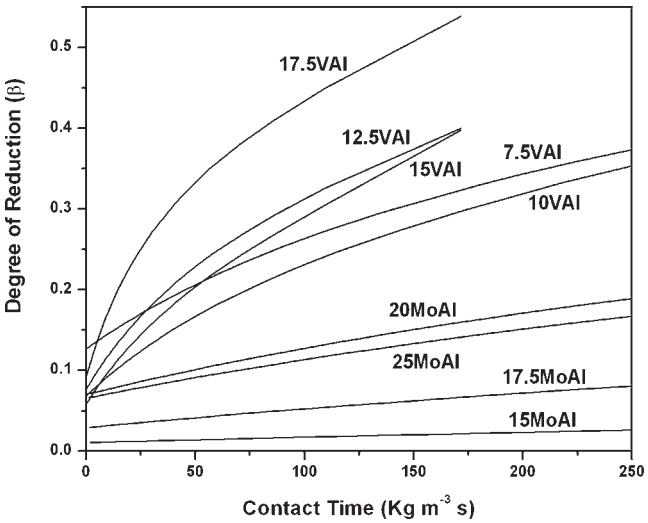

Figure 6. Variation of the degree of reduction with contact time for different catalysts at T = 653 K and C_3H_8:O_2 = 2:1.

ODH reaction. Furthermore, the contribution of β, which makes Eq. 5 nonfirst order, is also given in Table 3,

$$\text{where, Term I} = \frac{F_{A0}}{W^* P_{C_3H_{8,in}}} \int_0^\tau k_1 P_{C_3H_8} d\tau \qquad (12)$$

$$\text{Term II} = \frac{F_{A0}}{W^* P_{C_3H_{8,in}}} \int_0^\tau \beta k_1 P_{C_3H_8} d\tau \qquad (13)$$

$$\text{and, Activity (gmol/g s)} = \frac{F_{A0}}{W^* P_{C_3H_{8,in}}} \int_0^\tau r_1 d\tau = \text{Term I} - \text{Term II} \qquad (14)$$

where $P_{C3H8,in}$ is the inlet partial pressure of propane, in atm, τ is the contact time, in g cat $(mL)^{-1}$ min and F_{A0} is the inlet molar flow rate of propane, in gmol/s.

Thus, the degree of reduction has a noticeable contribution in describing the propane ODH reaction over these supported metal oxide catalysts and the reactions are ideally nonfirst order.

To compare the propene yield for the different catalysts it is important to consider variations in the ratio $k_1/(k_2+k_3)$.[24,33] Larger the value of $k_1/(k_2+k_3)$ higher is the propene yield at iso-conversion. Though the $k_1/(k_2+k_3)$ value is ideally suited for first order reactions, analysis of the propene yield at iso-conversion eliminates the dependency of the $(1-\beta)$ term. With the closeness of the E_2 and E_3 values the $k_1/(k_2+k_3)$ ratio can be approximated as

$$\frac{k_1}{k_2+k_3} = \frac{k_{10}}{k_{20}+k_{30}} \exp\left[-\frac{E_1 - E_{CO_x}}{R}\left(\frac{1}{T}-\frac{1}{T_m}\right)\right] \qquad (15)$$

where $E_{CO_x} = [1/2]\,(E_2+E_3)$

Thus, analysis of the variations in $k_1/(k_2+k_3)$ value primarily involves two factors: (i) the $k_{10}/(k_{20}+k_{30})$ ratio and (ii) the activation energy difference, $\Delta E = E_1 - E_{CO_x}$. The variations of these two factors with loading and specific surface metal oxide species are shown in Figures 7a, b. Note that in Figure 7 the metal oxide loading is converted to surface coverage, based on 15 wt % V_2O_5 and 20 wt % MoO_3 representing monolayer coverage. For the VAl catalysts the

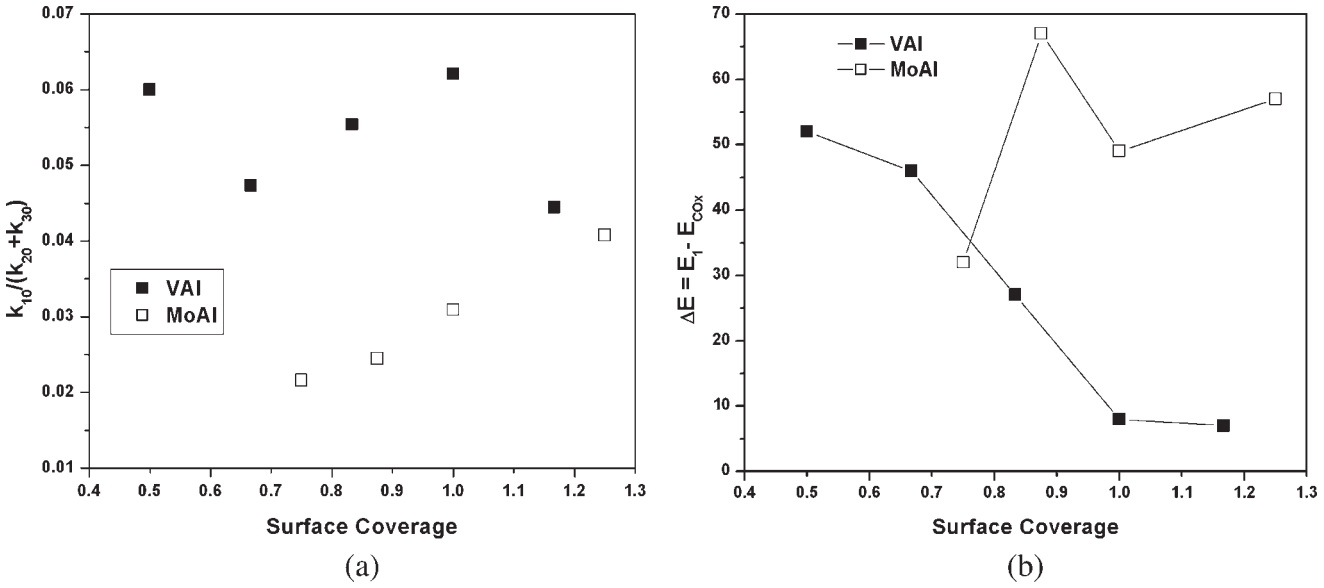

Figure 7. (a) Variation of the $k_{10}/(k_{20}+k_{30})$ ratio with surface coverage for VAl and MoAl samples; (b) variation of the activation energy difference between propene and carbon oxide formation with surface coverage for VAl and MoAl samples.

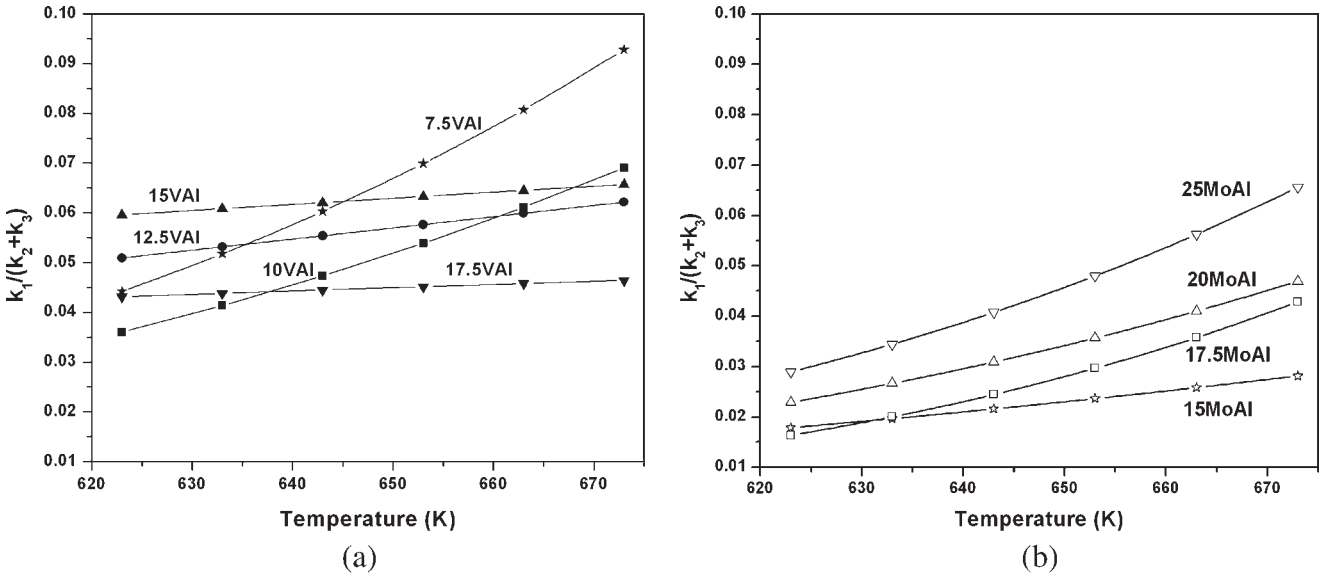

Figure 8. Effect of temperature on the $k_1/(k_2+k_3)$ ratio for (a) VAl samples and (b) MoAl samples.

$k_{10}/(k_{20}+k_{30})$ ratio varies between 0.045 and 0.062 with no specific trend with surface coverage and is higher than the values obtained for the MoAl samples. For the MoAl catalyst the ratio appears to increase with surface coverage from 0.022 to 0.041. The activation energy difference, ΔE value, progressively decreases as the vanadia loading is increased and approaches a constant value for near and above monolayer surface coverage. For the MoAl samples, however, the ΔE values are relatively constant. Since the activation energy (E_1) for propene formation is relatively constant for both catalytic systems, the variation of ΔE values reveals that the activation energy for carbon oxide formation (E_{CO_x}) does depend on the specific surface metal oxide species present. Furthermore, correlating the activation energy variation with structural information it would appear that the polymeric vanadia species possess higher activation energy for propene activation since they are preferentially present at high surface coverages.[5,41,52–54] However, the same relationship of structure-activation energy is not observed for the MoAl samples since the structure changes with loading and the activation energy for propene activation is similar.

On the basis of the kinetic parameters the $k_1/(k_2+k_3)$ value is calculated at different temperatures in Figures 8a, b for the VAl and MoAl catalysts, respectively. The results in Figures 8a, b reveal that the $k_1/(k_2+k_3)$ value increases with temperature due to the positive ΔE values. An increase in $k_1/(k_2+k_3)$ value with temperature suggests that an increase in propene yield at iso-conversion is achieved at high temperatures.[12,24] Specifically, the $k_1/(k_2+k_3)$ values for the VAl catalysts is larger at most temperatures. The larger $k_1/(k_2+k_3)$ values suggest that the propene yield at iso-conversion for the VAl catalysts is higher than those for the MoAl catalysts, which is consistent with the experimental results. Furthermore, no specific trend in $k_1/(k_2+k_3)$ value at a particular temperature is observed for the VAl catalysts as a function of loading, whereas for the MoAl catalysts the $k_1/(k_2+k_3)$ value increases with an increase in loading. For the VAl catalysts the $k_1/(k_2+k_3)$ versus temperature curves intersect since the $k_{10}/(k_{20}+k_{30})$ values does not show any specific trend and the ΔE values decrease with temperature. Thus, comparison of the propene yields for the VAl catalysts as a function of loadings is not straight-forward and depends on the particular temperature considered. In contrast, the MoAl catalysts reveal that at a particular temperature an increase in $k_1/(k_2+k_3)$ value with loading is observed even for samples above monolayer coverage since the $k_{10}/(k_{20}+k_{30})$ value increases with loading. Thus, the propene yield at iso-conversion: (i) increases with temperature (ii) at most temperatures higher for the VAl catalysts and (iii) does not increase with loading for the VAl catalysts, but increases with loading for the MoAl catalysts.

The variations of experimental and predicted propene yield with propane conversion for different C_3H_8 to O_2 molar ratios (1:1, 2:1, and 3:1) are shown in Figure 9 to study the

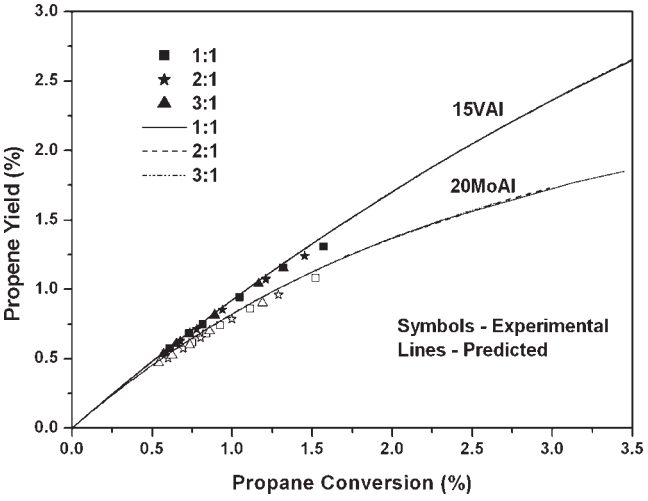

Figure 9. Effect of propane to oxygen molar ratio on propene yields at iso-conversion at T = 653 K.

effect of oxygen partial pressure on the propene yields. It is evident from Figure 9 that the C_3H_8 to O_2 molar ratio has no influence on the propene yield provided the comparison is done at iso-conversion. Similar behavior is also observed on other catalysts. In situ Raman and propane ODH studies over V_2O_5/Al_2O_3 catalysts have been shown that the C_3H_8 to O_2 molar ratio has no appreciable effect on the activity and selectivity of the catalysts.[7]

The effect of surface metal oxide phase and metal oxide loading on kinetic parameters associated with the re-oxidation reaction, k_{40} and E_4, is also observed. The k_{40} values of the VAl catalyst increase with vanadia loading up to monolayer coverage (15VAl) and decrease for 17.5VAl sample. However, for the MoAl catalysts the k_{40} values are relatively constant. Furthermore, the k_{40} values are significantly higher for the VAl catalysts compared to the MoAl catalysts. The re-oxidation activation energy, E_4, for both VAl and MoAl samples varies between 91 and 180 kJ/mol with no specific tend based on metal oxide loading and specific metal oxide phase. Thus, it appears that the redox rates strongly depend on the surface metal oxide species present on the oxide support and it is faster on the surface vanadium oxide species.

In summary, the surface vanadium and molybdenum oxide species present on the alumina support are catalytically different for the propane ODH reaction in terms of the propane conversion and propene yields. The surface vanadia species is more active than the surface molybdena species for the propane ODH reaction due to the different apparent pre-exponential factor and not the activation energy, and at iso-conversions requires a shorter contact time. Furthermore, the surface vanadia species also provide a higher propene yield at iso-conversions. These variations are explained in terms of changes in the apparent pre-exponential factors and activation energy.

Conclusions

The propane ODH reaction was carried out over supported V_2O_5/Al_2O_3 (VAl) and MoO_3/Al_2O_3 (MoAl) catalysts to understand the effect of metal oxide loading and specific surface metal oxide phase in terms of variations in kinetic parameters. Characterization studies reveal that below monolayer coverage only surface metal oxide species are present on the Al_2O_3 support. Above monolayer coverage bulk $AlVO_4$ and $Al_2(MoO_4)_3$ are also observed for the supported VAl and MoAl catalysts, respectively. The monolayer coverage based on the highest loading where bulk compounds are not formed corresponds to ~9.0 V and ~5.9 Mo atoms/nm^2 for the VAl and MoAl catalysts, respectively.

The kinetic parameters estimated for a sequential Mars–van Krevelen reaction model were able to predict the observed outlet concentrations successfully, suggesting proper representation of the reaction over these catalysts. The analysis of the kinetic parameters revealed that the apparent pre-exponential factors for the propane oxidation, $k_{10,}$ and propene oxidation reactions, k_{20} and k_{30}, increase monotonically with vanadia loading up to monolayer coverage for the VAl catalysts. For the MoAl catalysts, the k_{10} and k_{30} values increase with molybdena loading up to 20MoAl, where as the k_{20} value is relatively constant. However, the activation energy for propane oxidation, E_1, is relatively independent of metal oxide loading and specific surface metal oxide phase present on Al_2O_3. The ratio of primary oxidation rate constants or apparent pre-exponential factors correlates well with the trends in propane oxidation TOF which is invariant with surface metal oxide loading and depends on the specific metal oxide phase. However, the variation of degree of reduction needs to be considered for quantitative comparison. The degree of reduction makes the propene and carbon oxide formation reactions nonfirst order. Furthermore, the activation energies for propene oxidation or carbon oxides formation reactions, E_2 and E_3, increase with loading for the VAl catalysts, but are similar for the MoAl catalysts. This in turn affects the variation of $k_1/(k_2+k_3)$ ratio with temperature. The propene yields at iso-conversion are generally higher for the VAl catalysts than the MoAl catalysts due to higher $k_1/(k_2+k_3)$ values of the VAl catalysts. Additionally, the propene yields at iso-conversion are relatively independent of loading for the VAl catalysts, but increase with loading for the MoAl catalysts.

Acknowledgments

The authors acknowledge the assistance of Prof. Israel E. Wachs, Lehigh University and Ms. Brishti Mitra, U.I.E.T, CSJM University, Kanpur, for providing the Raman data and Ms. M. De and Mr. D. Shee of IIT Kanpur for assistance with the TPR experiments.

Literature Cited

1. Kung HH. Oxidative dehydrogenation of light (C_2 to C_4) alkanes. *Adv Catal*. 1995;40:1–38.
2. Mamedov EA, Corberan VC. Oxidative dehydrogenation of lower alkanes on vanadium oxide-based catalysts. The present state of the art and outlooks. *Appl Catal A*. 1995;127:1–40.
3. Cavani F, Trifiro F. The oxidative dehydrogenation of ethane and propane as an alternative way for the production of light olefins. *Catal Today*. 1995;24:307–313.
4. Blasco T, Nieto JML. Oxidative dehydrogenation of short chain alkanes on supported vanadium oxide catalysts. *Appl Catal A*. 1997; 157:117–142.
5. Wachs IE, Weckhuysen BM. Structure and reactivity of surface vanadium oxide species on oxide supports. *Appl Catal A*. 1997;157:67–90.
6. Christodoulakis A, Machli M, Lemonidou AA, Boghosian S. Molecular structure and reactivity of vanadia-based catalysts for propane oxidative dehydrogenation studied by in situ Raman spectroscopy and catalytic activity measurements. *J Catal*. 2004;222:293–306.
7. Cortez GG, Banares MA. A Raman spectroscopy study of alumina-supported vanadium oxide catalyst during propane oxidative dehydrogenation with online activity measurement. *J Catal*. 2002;209: 197–201.
8. Gao X, Jehng JM, Wachs IE. In situ UV-vis-NIR diffuse reflectance and Raman spectroscopic studies of propane oxidation over ZrO_2-supported vanadium oxide catalysts. *J Catal*. 2002;209:43–50.
9. Martra G, Arena F, Coluccia S, Frusteri F, Parmaliana A. Factors controlling the selectivity of V_2O_5 supported catalysts in the oxidative dehydrogenation of propane. *Catal Today*. 2000;63:197–207.
10. Chen K, Khodakov A, Yang J, Bell AT, Iglesia E. Isotopic tracer and kinetic studies of oxidative dehydrogenation pathways on vanadium oxide catalysts. *J Catal*. 1999;186:325–333.
11. Kondratenko EV, Cherian M, Baerns M. Mechanistic aspects of the oxidative dehydrogenation of propane over an alumina-supported $VCrMnWO_x$ mixed oxide catalyst. *Catal Today*. 2005;99:59–67.
12. Routray K, Reddy KRSK, Deo G. Oxidative dehydrogenation of propane on V_2O_5/Al_2O_3 and V_2O_5/TiO_2 catalysts: understanding the effect of support by parameter estimation. *Appl Catal A*. 2004;265:103–113.
13. Argyle MD, Chen K, Bell AT, Iglesia E. Effect of catalyst structure on oxidative dehydrogenation of ethane and propane on alumina-supported vanadia. *J Catal*. 2002;208:139–149.

14. Khodakov A, Olthof B, Bell AT, Iglesia E. Structure and catalytic properties of supported vanadium oxides: support effects on oxidative dehydrogenation reactions. *J Catal*. 1999;181:205–216.
15. Eon JG, Olier R, Volta JC. Oxidative dehydrogenation of propane on γ-Al_2O_3 supported vanadium oxides. *J Catal*. 1994;145:318–326.
16. Kondratenko EV, Baerns M. Catalytic oxidative dehydrogenation of propane in the presence of O_2 and N_2O-the role of vanadia distribution and oxidant activation. *Appl Catal A*. 2001;222:133–143.
17. Bottino A, Capannelli G, Comite A, Storace S, Felice RD. Kinetic investigations on the oxidehydrogenation of propane over vanadium supported on γ-Al_2O_3. *Chem Eng J*. 2003;94:11–18.
18. Lemonidou AA, Nalbandian L, Vasalos IA. Oxidative dehydrogenation of propane over vanadium oxide based catalysts: effect of support and alkali promoter. *Catal Today*. 2000;61:333–341.
19. Heracleous E, Machli M, Lemonidou AA, Vasalos IA. Oxidative dehydrogenation of ethane and propane over vanadia and molybdena supported catalysts. *J Mol Catal A*. 2005;232:29–39.
20. Chen K, Xie S, Bell AT, Iglesia E. Structure and properties of oxidative dehydrogenation catalysts based on MoO_3/Al_2O_3. *J Catal*. 2001;198:232–242.
21. Meunier FC, Yasmeen A, Ross JRH. Oxidative dehydrogenation of propane over molybdenum-containing catalysts. *Catal Today*. 1997; 37:33–42.
22. Abello MC, Gomez MF, Ferretti O. Mo/γ-Al_2O_3 catalysts for the oxidative dehydrogenation of propane.: effect of Mo loading. *Appl Catal A*. 2001;207:421–431.
23. Routray K, Deo G. Kinetic parameter estimation for a multiresponse nonlinear reaction model. *AIChE J*. 2005;51:1733–1746.
24. Singh RP, Banares MA, Deo G. Effect of phosphorous modifier on V_2O_5/TiO_2 catalyst: ODH of propane. *J Catal*. 2005;233:388–398.
25. Creaser D, Andersson B, Hudgins RR, Silveston PL. Transient kinetic analysis of the oxidative dehydrogenation of propane. *J Catal*. 1999;182:264–269.
26. Creaser D, Andersson B. Oxidative dehydrogenation of propane over V-Mg-O: kinetic investigation by nonlinear regression analysis. *Appl Catal A*. 1996;141:131–152.
27. Grabowski R. Kinetics of the oxidative dehydrogenation of propane on vanadia/titania catalysts, pure and doped with rubidium. *Appl Catal A*. 2004;270:37–47.
28. Grabowski R, Grzybowska B, Samson K, Sloczynski J, Stoch J, Weislo K. Effect of alkaline promoters on catalytic activity of V_2O_5/TiO_2 and MoO_3/TiO_2 catalysts in oxidative dehydrogenation of propane and in isopropanol decomposition. *Appl Catal A*. 1995;125: 129–144.
29. Watling TC, Deo G, Seshan K, Wachs IE, Lercher JA. Oxidative dehydrogenation of propane over niobia supported vanadium oxide catalysts. *Catal Today*. 1996;28:139–145.
30. Shee D, Rao TVM, Deo G. Kinetic parameter estimation for supported vanadium oxide catalysts for propane ODH reaction: effect of loading and support. *Catal Today*. 2006;118:288–297.
31. Tian H, Ross EI, Wachs IE. Quantitative determination of the speciation of surface vanadium oxides and their catalytic activity. *J Phys Chem B*. 2006;110:9593–9600.
32. Rao TVM, Deo G, Jehng JM, Wachs IE. In situ UV-vis-NIR diffuse reflectance and Raman spectroscopy and catalytic activity studies of propane oxidative dehydrogenation over supported CrO_3/ZrO_2 catalysts. *Langmuir*. 2004;20:7159–7165.
33. Fogler HS. Elements of Chemical Reaction Engineering, 3rd ed. New Delhi: Prentice-Hall of India, 2002.
34. Froment GF, Bischoff KB. Chemical Reactor Analysis and Design, 2nd ed. New York: Wiley, 1990.
35. Mars P, van Krevelen DW. Oxidations carried out by means of vanadium oxide catalysts. *Chem Eng Sci*. 1954;3(Spec Suppl):41–59.
36. Haber J, Turek W. Kinetic studies as a method to differentiate between oxygen species involved in the oxidation of propene. *J Catal*. 2000;190:320–326.
37. Rao TVM, Deo G. Ethane and propane oxidation over supported V_2O_5/TiO_2 catalysts: analysis of kinetic parameters. *Ind Eng Chem Res*. 2007;46:70–79.
38. Rao TVM, Deo G. Steady state kinetic parameters of bulk V_2O_5 for ethane and propane oxidation reactions. *Catal Commun*. 2007;8: 957–962.
39. Deo G, Cherian M, Rao TVM. Oxidative dehydrogenation (ODH) of alkanes over metal oxide catalysts. In: Fierro JLG, editor. Metal Oxides: Chemistry and Applications. New York: CRC, 2006:491–516.
40. Deo G, Hardcastle FD, Richards M, Hirt AM, Wachs IE. In: Baker RTK, Murrell LL, editors. Novel Materials in Heterogeneous catalysis (ACS Symposium Series, Vol. 437). Washington, DC: American Chemical Society, 1990:317.
41. Magg N, Immaraporn B, Giorgi JB, Schroeder T, Bäumer M, Döbler J, Wu Z, Kondratenko E, Cherian M, Baerns M, Stair PC, Sauer J, Freund H-J. Vibrational spectra of alumina- and silica-supported vanadia revisited: an experimental and theoretical model catalyst study. *J Catal*. 2004;226:88–100.
42. Kanervo JM, Harlin ME, Krause AOI, Banares MA. Characterization of alumina-supported vanadium oxide catalysts by kinetic analysis of H_2-TPR data. *Catal Today*. 2003;78:171–180.
43. Briand LE, Jehng JM, Cornaglia L, Hirt AM, Wachs IE. Quantitative determination of the number of surface active sites and the turnover frequency for methanol oxidation over bulk metal vanadates. *Catal Today*. 2003;78:257–268.
44. Hu H, Bare SR, Wachs IE. Surface structures of supported molybdenum oxide catalysts: characterization by Raman and Mo L3-Edge XANES. *J Phys Chem*. 1995;99:10897–10910.
45. Briand LE, Hirt AM, Wachs IE. Quantitative determination of the number of surface active sites and the turnover frequencies for methanol oxidation over metal oxide catalysts: application to bulk metal molybdates and pure metal oxide catalysts. *J Catal*. 2001;202:268–278.
46. Wachs IE, Hardcastle FD, Chan SS. Characterization of supported metal oxides by laser Raman spectroscopy: supported vanadium oxide on alumina and titania. *Mat Res Soc Symp Proc*. 1988;111:353–358.
47. Said AA. Mutual influences between ammonium heptamolybdate and γ-alumina during their thermal treatments. *Thermochim Acta*. 1994;236:93–104.
48. Wachs IE. Raman and IR studies of surface metal oxide species on oxide supports: supported metal oxide catalysts. *Catal Today*. 1996;27;437–455.
49. Yao HC. Surface interaction in the MoO_3/γ-Al_2O_3 system. *J Catal*. 1981;70:440–444.
50. Arnoldy P, De Jonge JCM, Moulijn JA. Temperature-programmed reduction of molybdenum(VI) oxide and molybdenum(IV) oxide. *J Phys Chem*. 1985;89:4517–4526.
51. Chen K, Bell AT, Iglesia E. The relationship between the electronic and redox properties of dispersed metal oxides and their turnover rates in oxidative dehydrogenation reactions. *J Catal*. 2002;209:35–42.
52. Vuurman MA, Wachs IE. In situ Raman spectroscopy of alumina-supported metal oxide catalysts. *J Phys Chem*. 1992;96:5008–5016.
53. Olthof B, Khodakov A, Bell AT, Iglesia E. Effects of support composition and pretreatment conditions on the structure of vanadia dispersed on SiO_2, Al_2O_3, TiO_2, ZrO_2, and HfO_2. *J Phys Chem B*. 2000;104:1516–1528.
54. Deo G, Wachs IE, Haber J. Supported vanadium oxide catalysts: molecular and structural characterization and reactivity properties. *Crit Rev Surf Chem*. 1994;4:141–187.

Manuscript received Oct. 26, 2006, and revision received Mar. 6, 2007.